

“Trampoline” ejection of organic molecules from graphene and graphite via keV cluster ions impacts

Stanislav V. Verkhoturov, Mikołaj Gołuński, Dmitriy S. Verkhoturov, Sheng Geng, Zbigniew Postawa, and Emile A. Schweikert

Citation: *The Journal of Chemical Physics* **148**, 144309 (2018); doi: 10.1063/1.5021352

View online: <https://doi.org/10.1063/1.5021352>

View Table of Contents: <http://aip.scitation.org/toc/jcp/148/14>

Published by the [American Institute of Physics](#)

Articles you may be interested in

[Microsolvation of phthalocyanine molecules in superfluid helium nanodroplets as revealed by the optical line shape at electronic origin](#)

The Journal of Chemical Physics **148**, 144301 (2018); 10.1063/1.5022006

[High-resolution infrared spectroscopy of \$O_2H^+\$ in a cryogenic ion trap](#)

The Journal of Chemical Physics **148**, 144303 (2018); 10.1063/1.5023633

[The dependency of adhesion and friction on electrostatic attraction](#)

The Journal of Chemical Physics **148**, 144701 (2018); 10.1063/1.5024038

[Force-detected nanoscale absorption spectroscopy in water at room temperature using an optical trap](#)

The Journal of Chemical Physics **148**, 144201 (2018); 10.1063/1.5017853

[A molecular dynamics investigation of the surface tension of water nanodroplets and a new technique for local pressure determination through density correlation](#)

The Journal of Chemical Physics **148**, 144503 (2018); 10.1063/1.5004985

[Relationship between x-ray emission and absorption spectroscopy and the local H-bond environment in water](#)

The Journal of Chemical Physics **148**, 144507 (2018); 10.1063/1.5009457

PHYSICS TODAY

WHITEPAPERS

ADVANCED LIGHT CURE ADHESIVES

Take a closer look at what these environmentally friendly adhesive systems can do

READ NOW

PRESENTED BY
 MASTERBOND[®]
ADHESIVES | SEALANTS | COATINGS

“Trampoline” ejection of organic molecules from graphene and graphite via keV cluster ions impacts

Stanislav V. Verkhoturov,¹ Mikołaj Gołuński,² Dmitriy S. Verkhoturov,¹ Sheng Geng,¹ Zbigniew Postawa,² and Emile A. Schweikert^{1,a)}

¹Department of Chemistry, Texas A&M University, College Station, Texas 77843-3144, USA

²Department of Physics, Jagiellonian University, Kraków, Poland

(Received 3 January 2018; accepted 27 March 2018; published online 12 April 2018)

We present the data on ejection of molecules and emission of molecular ions caused by single impacts of 50 keV C_{60}^{2+} on a molecular layer of deuterated phenylalanine (D8Phe) deposited on free standing, 2-layer graphene. The projectile impacts on the graphene side stimulate the abundant ejection of intact molecules and the emission of molecular ions in the transmission direction. To gain insight into the mechanism of ejection, Molecular Dynamic simulations were performed. It was found that the projectile penetrates the thin layer of graphene, partially depositing the projectile's kinetic energy, and molecules are ejected from the hot area around the hole that is made by the projectile. The yield, Y , of negative ions of deprotonated phenylalanine, $(D8Phe-H)^-$, emitted in the transmission direction is 0.1 ions per projectile impact. To characterize the ejection and ionization of molecules, we have performed the experiments on emission of $(D8Phe-H)^-$ from the surface of bulk D8Phe ($Y = 0.13$) and from the single molecular layer of D8Phe deposited on bulk pyrolytic graphite ($Y = 0.15$). We show that, despite the similar yields of molecular ions, the scenario of the energy deposition and ejection of molecules is different for the case of graphene due to the confined volume of projectile-analyte interaction. The projectile impact on the graphene-D8Phe sample stimulates the collective radial movement of analyte atoms, which compresses the D8Phe layer radially from the hole. At the same time, this compression bends and stretches the graphene membrane around the hole thus accumulating potential energy. The accumulated potential energy is transformed into the kinetic energy of correlated movement upward for membrane atoms, thus the membrane acts as a trampoline for the molecules. The ejected molecules are effectively ionized; the ionization probability is $\sim 30\times$ higher compared to that obtained for the bulk D8Phe target. The proposed mechanism of ionization involves tunneling of electrons from the vibrationally excited area around the hole to the molecules. Another proposed mechanism is a direct proton transfer exchange, which is suitable for a bulk target: ions of molecular fragments (i.e., CN^-) generated in the impact area interact with intact molecules from the rim of this area. There is a direct proton exchange process for the system D8Phe molecule + CN^- . *Published by AIP Publishing.* <https://doi.org/10.1063/1.5021352>

INTRODUCTION

Secondary ion mass spectrometry, SIMS, is well recognized as a highly sensitive surface analysis technique.¹ The secondary ion, SI, emission process is explained as the result of the dissipation of the projectile kinetic energy via linear collision cascades (atomic projectiles) or high density collision cascades in the case of cluster impacts.² The high density cascades in turn generate correlated pulses toward the surface around the impact crater promoting the sputtering of neutral and emission of ionized species as atoms, molecules and molecular fragments. The full development of the collision cascades assumes a solid of at least 100 nm in thickness. However, in a departure from the conventional SIMS experiment, we have observed abundant emission of small carbon clusters, when bombarding free-standing graphene with C_{60}^{2+}

or Au_{400}^{4+} at hypervelocities.^{3,4} The emissions referred to here are in a transmission (forward) direction. Further experiments, where a single layer of C_{60} deposited on free-standing graphene was bombarded with 50 keV C_{60}^{2+} , showed that the yield of C_{60}^- emitted in the transmission direction is comparable to that obtained from a monolayer of C_{60} on pyrolytic graphite, and even comparable to that from a bulk C_{60} deposit.⁵ In the latter cases, bombardment was also with 50 keV C_{60}^{2+} , but the C_{60}^- emission was measured in the conventional reflection direction. Clearly, the C_{60} on the 2D substrate is ejected and ionized with high efficiency, in a mode that differs from the conventional SIMS process. Molecular dynamics (MD) simulations of C_{60} bombarding a monolayer of C_{60} deposited on two layers of free standing graphene show that intact C_{60} is ejected within a few ps from a “hot” vibrationally excited rim around the impact rupture.⁵ The proposed mechanism of ejection involves a combination of an “evaporation” process from the vibrationally excited area, with a kinetic repulsion process due to the graphene membrane oscillating around the

^{a)}Electronic mail: schweikert@tamu.edu

impact hole. The high degree of ionization of the ejected C_{60} may be explained as due to electron tunneling between the hot graphene and the ejecta.

The question now arises if the efficient ejection-ionization observed for C_{60} occurs also for organic molecules in monolayer deposit on graphene. We address this issue here with a study on SI emission from monolayer deposits of phenylalanine on graphene under C_{60} bombardment. The observations are compared with data from monolayer and bulk deposits of the same analyte on bulk graphite. For the additional insight, the findings are compared with MD simulations run on equivalent samples and conditions.

EXPERIMENTAL

Instrumentation

The experiments were run with a custom-built cluster-SIMS instrument consisting of two identical C_{60} effusion sources (Fig. 1). One cluster ion source generates 50 keV C_{60}^{2+} projectiles which impact the back side of a thin target (e.g., graphene) at an angle of incidence of 0° from normal. This setup is used for the detection of secondary ions which are emitted in the transmission direction. Another C_{60} source is used for impacts on the front side of the bulk target at an angle of incidence of 25° from normal. The secondary ions are emitted/detected in the reflection direction. The SIMS instrument is equipped with a 1.2 m linear time-of-flight mass spectrometer, ToF-MS, and an electron emission microscope, EEM.^{6,7} The EEM was used here solely to detect secondary electrons for the ToF start signal. The data were acquired at the level of individual C_{60} impacts with a repetition rate of 1000 impacts/s. This event-by-event bombardment-detection mode allows us to select specific impacts, in the present case those involving free-standing graphene,³ at the exclusion of signals from the target holder and support. A detailed description of the components and data acquisition processing scheme can be found elsewhere.⁷

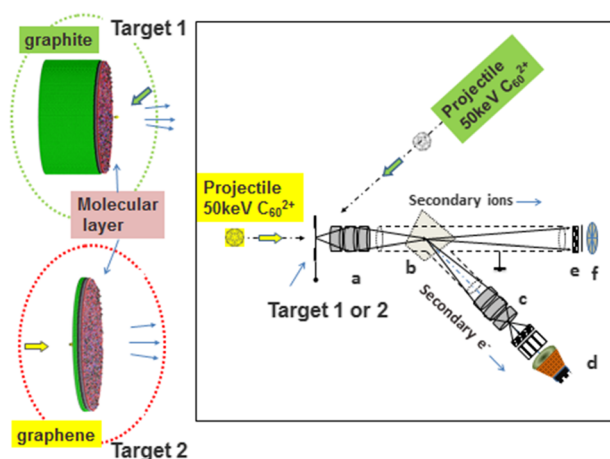


FIG. 1. Schematic of experiment: (a) objective lens for secondary ions and electrons, (b) magnetic prism for the redirection of electrons toward imaging electron optics (c), (c) imaging electron optics, (d) position sensitive detector consisting of dual microchannel plate, phosphor screen, and CMOS camera, (e) dual microchannel plate, and (f) 8 anode detector.

Samples

A layer of deuterated phenylalanine (D8Phe) molecules (Fig. 1) was vapor deposited on 2-layer graphene or pyrolytic graphite. The graphene was supported by a lacey carbon film on a copper TEM grid with 300 lines/in. (Ted Pella, Inc., Redding, CA). The support was analyzed and the contribution of the observed SIs from the lacey carbon was found to be small.³ The pyrolytic graphite plate of thickness of 0.5 mm (Sigma Aldrich, Inc.) has 99.99% purity.

The deposition of D8Phe was made in high vacuum with a growth rate of the molecular layer of 50 nm/min. The time of deposition was controlled with a shutter placed in front of the sample. A one second exposure time resulted in a single molecular layer of ~ 1 nm thickness.

Homogeneity test

The uniformity of the D8Phe layer was tested using event-by-event bombardment-detection mode.⁶ The method allows us to detect the $(D8Phe-H)^-$ ions that are co-emitted with the D^- ions and compute the correlation coefficients of co-emission⁸

$$K_n = \frac{Y_{D,Phe}}{Y_D Y_{Phe}}, \quad (1)$$

where Y_D and Y_{Phe} are the yields (the number of emitted ions that are detected per projectile impact) of $(D8Phe-H)^-$ ions and D^- ions, respectively, and $Y_{D,Phe}$ is the yield of co-emitted $(D8Phe-H)^-$ and D^- ions.

For the homogeneous surface, the ions are emitted independently from any point of the impacting area.⁸ Thus, for the homogeneous surface, $K_n = 1$.

The measured yields are given by

$$Y_{Phe} = I_{Phe}/N_{eff}, \quad (2)$$

$$Y_D = I_D/N_{eff}, \quad (3)$$

$$Y_{D,Phe} = I_{D,Phe}/N_{eff}, \quad (4)$$

where I_{Phe} is the number of detected $(D8Phe-H)^-$, I_D is the number of detected D^- , $I_{D,Phe}$ is the number of detected co-emitted ions and N_{eff} is the effective number of impacts on the area of the target, which is covered by the molecular layer.

Using the expressions (1)–(4), one can obtain N_{eff} ,

$$N_{eff} = \frac{I_D I_{Phe}}{I_{D,Phe}}. \quad (5)$$

If the molecular coverage of the surface is incomplete, the effective number of impacts is less than the total number of impacts, N_0 ,

$$N_{eff} < N_0. \quad (6)$$

To compare the quality of the D8Phe layers deposited on different substrates, the degree of coverage can be written in the form as

$$\alpha (100\%) = \frac{N_{eff}}{N_0} 100\%. \quad (7)$$

The degree of coverage, α , the yields of $(D8Phe-H)^-$, Y_{Phe} and other measured ions for the different targets are presented in Table I.

The degrees of coverage, presented in Table I, show that the Targets I and II are well covered by D8Phe molecules. The

TABLE I. Degree of coverage, α , yield of $(\text{D8Phe-H})^-$, Y_{Phe} , and the yields of some atomic and fragment negative ions measured for different targets. (Target I) 2-layer graphene coated by ~ 1 nm layer of D8Phe. The projectiles impact graphene first; the emitted ions are detected in the transmission direction. (Target II) Bulk pyrolytic graphite coated by ~ 1 nm layer of D8Phe. (Target III) Thick layer (~ 500 nm) of D8Phe deposited on pyrolytic graphite. A thickness of 500 nm is enough to consider this target as bulk D8Phe. For the Targets II and III, the projectiles impact first the D8Phe layer; the emitted ions are detected in the reflection direction. The standard deviation is better than $\pm 5\%$ for all values of the experimental α .

	α (%)	Y_{Phe}	Y_{D}	Y_{C_1}	Y_{CN}	Y_{CD}	Y_{OD}	Y_{O}
Target I	89	0.10	0.10	0.15	0.31	0.04	0.02	0.12
Target II	86	0.15	0.06	0.03	0.22	0.02	0.01	0.04
Target III	100	0.13	0.11	0.04	0.23	0.03	0.01	0.04

thickness of the layer is ~ 1 nm (50 nm/min deposition rate with an exposure time of 1 s). The coverages were 89% and 86% for the Targets I and II, respectively.

Molecular dynamics simulations

The molecular dynamics (MD) computer simulations were used to investigate processes leading to material ejection from a graphene substrate covered with a phenylalanine overlayer bombarded by C_{60} projectiles. Briefly, the movement of particles is determined by integrating Hamilton's equations of motion. Targets consisting of one layer of phenylalanine (Phe) deposited on 2 layers and 30 layers of graphene are shown in Fig. 2. A detailed description of the MD method can be found elsewhere.⁹ The cylindrical samples are selected based on visual observations of energy transfer pathways stimulated by impacts of C_{60} projectiles. The sample diameter was chosen to minimize edge effects associated with the dynamic events leading to ejection of particles. The graphene substrates had a circular shape with a radius of 20 nm and a thickness of approximately 0.34 nm and 5.1 nm, containing 92 162 and 1 382 430 carbon atoms, respectively. The phenylalanine monolayer, consisting of 5013 molecules or 115 299 atoms, was deposited on graphene and re-equilibrated to achieve

a configuration with minimal potential energy. This procedure resulted in a monolayer approximately 1.11 nm thick. The phenylalanine multilayer was represented by 10 layers of phenylalanine deposited on two layers of graphene. This system consisted of 50 317 molecules or 1 157 291 atoms. One should note that in MD simulations, the Phe molecules are not deuterated. The slight difference in bond strength between D8Phe and Phe is of no concern here. Reactive force field (ReaxFF) potential splined at a short distance with the Ziegler-Biersack-Littmark (ZBL) potential to properly describe high energy collisions was used to describe interactions among all atoms in the system.¹⁰

Rigid and stochastic regions around the edge of the sample were used to preserve sample shape and prevent back reflection of the waves generated by the projectile impact from back reflection from the system boundary.¹¹ We found that the tooth-sawtooth shape of the stochastic zone (like in breakwaters) is more effective for eliminating constructive interference of energy waves that reflect from the boundaries than a simpler cylindrically shaped zone. The C_{60} projectile is situated "below" the sample in a "transmission" setup for a 2-layer graphene substrate [Fig. 2(a)]. Thus the detected molecules are ejected on the other side of the sample than the side that is hit by a projectile. The projectile is located above the substrate in a "reflection" configuration for a 30-layer graphene system [Fig. 2(b)]. In this case, molecules are emitted in the direction opposite to the initial projectile movement. The atoms in the target have initially zero velocity. The atoms in the C_{60} projectile have initially no velocity relative to the center of mass motion. The C_{60} projectiles with a kinetic energy of 50 keV are directed along the surface normal.

The simulations are run in a NVE ensemble and extend up to 60 ps, which is long enough to achieve saturation in the ejection yield vs time dependence. Nine randomly selected impact points located near the center of the sample are chosen to achieve statistically reliable data. Simulations are performed with the Large-scale Atomic/Molecular Massively Parallel Simulator (LAMMPS) code,¹² which was modified to better describe sputtering conditions.

RESULTS AND DISCUSSION

The mass spectra of negative ions emitted from different targets (Targets I-III) are shown in Figs. 3–5, respectively.

All mass spectra of emitted negative ions contain peaks of D8Phe fragment ions of C_n^- , C_nH^- , C_nD^- ($n \leq 10$), OH^- , OD^- , and O^- (Figs. 3–5). The presence of O^- and C_nH_x^- in the spectra also implies that the graphene as well as pyrolytic graphite is partially oxidized and has contaminants due to exposure in air prior to the experiments in a vacuum.³

While the mass spectra of all targets appear to be similar, there are a few notable differences. The first difference is the high yield of C_1^- in the transmission experiments (Target I), which is in part attributed to fragmentation and atomization of the projectile after impact followed by the ionization of the projectile's carbon atoms. Indeed, the yields of C_1^- measured for the reflection direction (bulk targets II and III) are much lower due to fewer recoiled projectile atoms. For Target I,

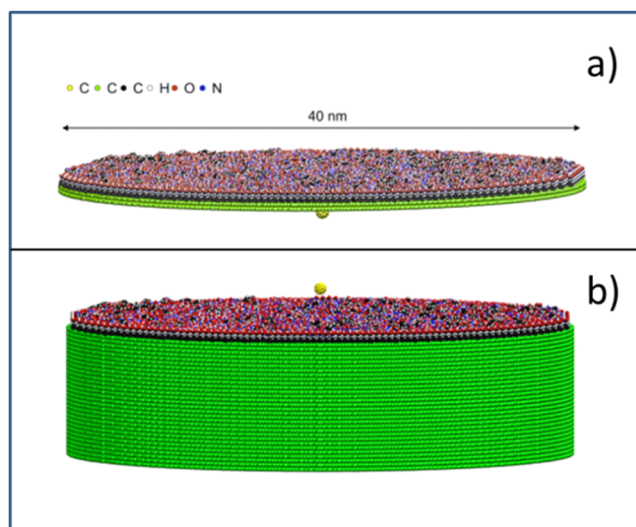


FIG. 2. Visualization of the atomic system used in simulations.

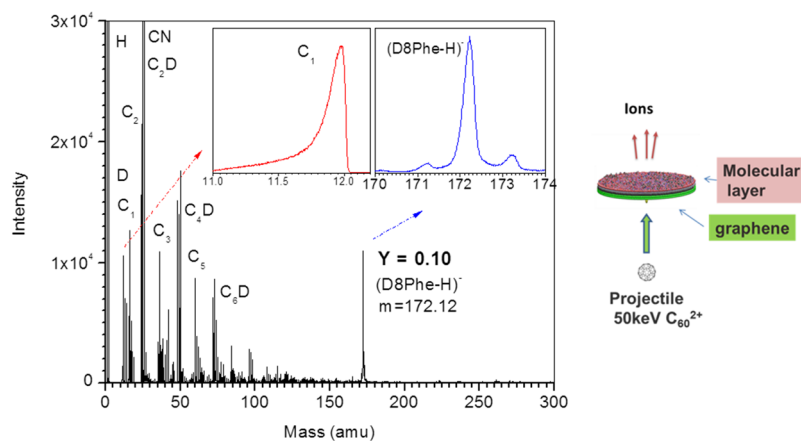


FIG. 3. Mass spectrum of negative ions emitted from the Target I (2-layer graphene coated by the molecular layer of D8Phe). The directions of bombardment and emission are shown in the sketch presented on the right-hand side of the figure.

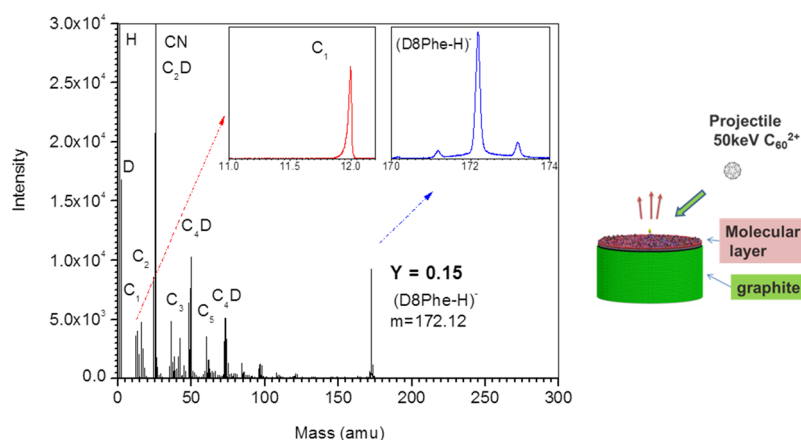


FIG. 4. Mass spectrum of negative ions emitted from the Target II (bulk pyrolytic graphite coated by the molecular layer of D8Phe). The directions of bombardment and emission are shown in the sketch presented on the right-hand side of the figure.

the shape of the C_1^- peak has an extended tail toward the low mass range, which indicates the presence of ions with high kinetic energies (discussed below). A further difference is the shape of the peak of $(D8Phe-H)^-$, which depends on mechanism/s of molecule ejection and ionization (discussed below).

The shape of the C_1^- peak can be converted into the kinetic energy distribution. Details of the measurement of the kinetic energy distributions are given in the supplementary material of Ref. 3.

The kinetic energy distributions of C_1^- are different for transmission and reflection experiments (Fig. 6). For the transmission experiments, the kinetic energies of C_1^- extend up to

1/60 (833 eV) of the projectile energy. This energy corresponds to the energy of projectile C atoms, or to the energy of C atoms, which are knocked on in a direct collision between projectile C atoms and C atoms of the D8Phe+graphene film. For the bulk target, the kinetic energies of C_1^- extend up to ~60–75 eV. These energies correspond to the energies of the C recoils, which are generated via collision cascades.²

Phenylalanine monolayer on graphene

A key finding is the abundant emission of deprotonated molecular ions of D8Phe from the molecular layer of D8Phe deposited on 2-layer graphene. The yield of 0.1 ions/impact

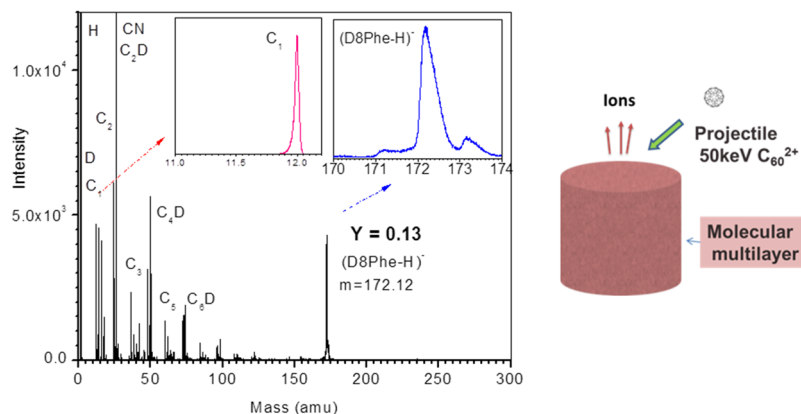


FIG. 5. Mass spectrum of negative ions emitted from the Target III (bulk D8Phe). The directions of bombardment and emission are shown in the sketch presented on the right-hand side of the figure.

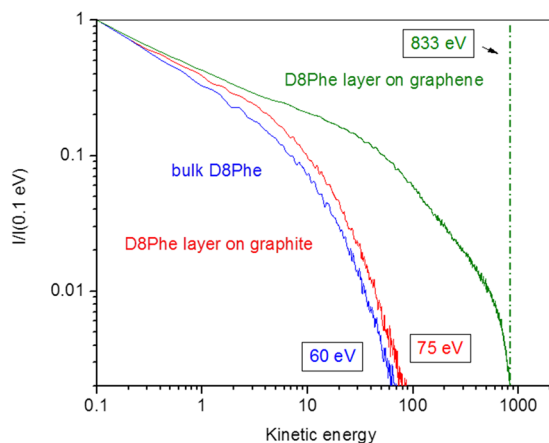


FIG. 6. Kinetic energy distributions measured for the atomic ions C_1^- emitted from the single molecular layer of D8Phe deposited on 2-layer graphene (green color, Target I), the single molecular layer of D8Phe deposited on pyrolytic graphite (red color, Target II) and bulk D8Phe (blue color, Target III).

is comparable with the yield for $(D8Phe-H)^-$ emitted from the bulk target (0.13 ions/impact). As noted earlier, projectile

impacts on bulk matter result in high density collision cascades, which are an efficient source for sputtering of intact molecules.²

In the case of 50 keV C_{60}^{2+} impacts on graphene covered with a monolayer of D8Phe, the C atoms of the projectile collide with those of the target. The knocked-on atoms carry a part of the kinetic energy of the projectile atoms. Another part of the kinetic energy is deposited into the rim around the impact site. MD simulations show that the molecules are ejected from this area (Figs. 7 and 8) (Multimedia view). Figure 7 (Multimedia view) shows the cut view and Fig. 8 (Multimedia view) shows the side view of the processes of Phe+graphene evolution and molecule ejection. The critical process, which regulates the abundance of the ejecta, is the separation of the molecular layer from graphene. The molecular layer evolves as a collective movement of Phe molecules and simultaneously the graphene oscillates downward/upward. The key step of molecule ejection occurs within first 2 ps after impact. The initial atom-atom interactions stimulated by the projectile impact are transformed into a collective radial movement of atoms of Phe molecules, which compresses the molecular layer

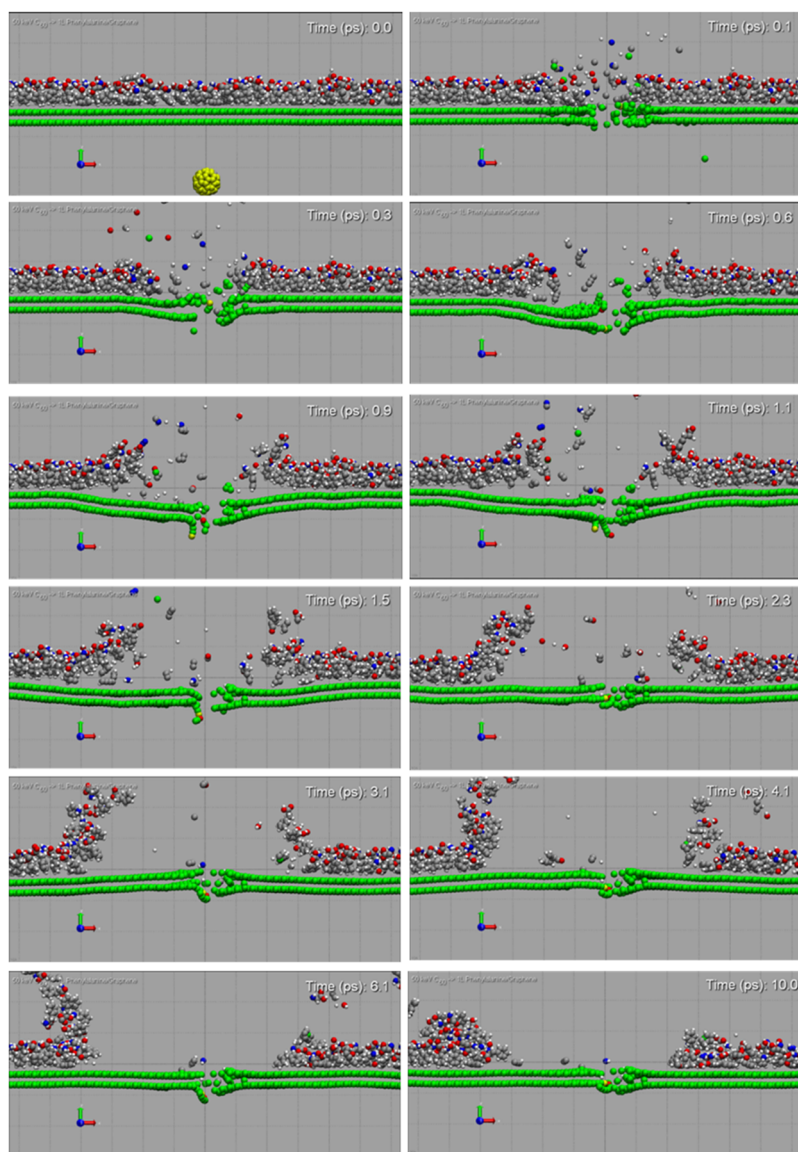


FIG. 7. Snapshots of the model system consisting of the single layer of phenylalanine molecules (1.1 nm) deposited on 2L graphene taken at various moments after 50 keV C_{60} impact—cross-sectional view. The corresponding movie file is here. Multimedia view: <https://doi.org/10.1063/1.5021352.1>

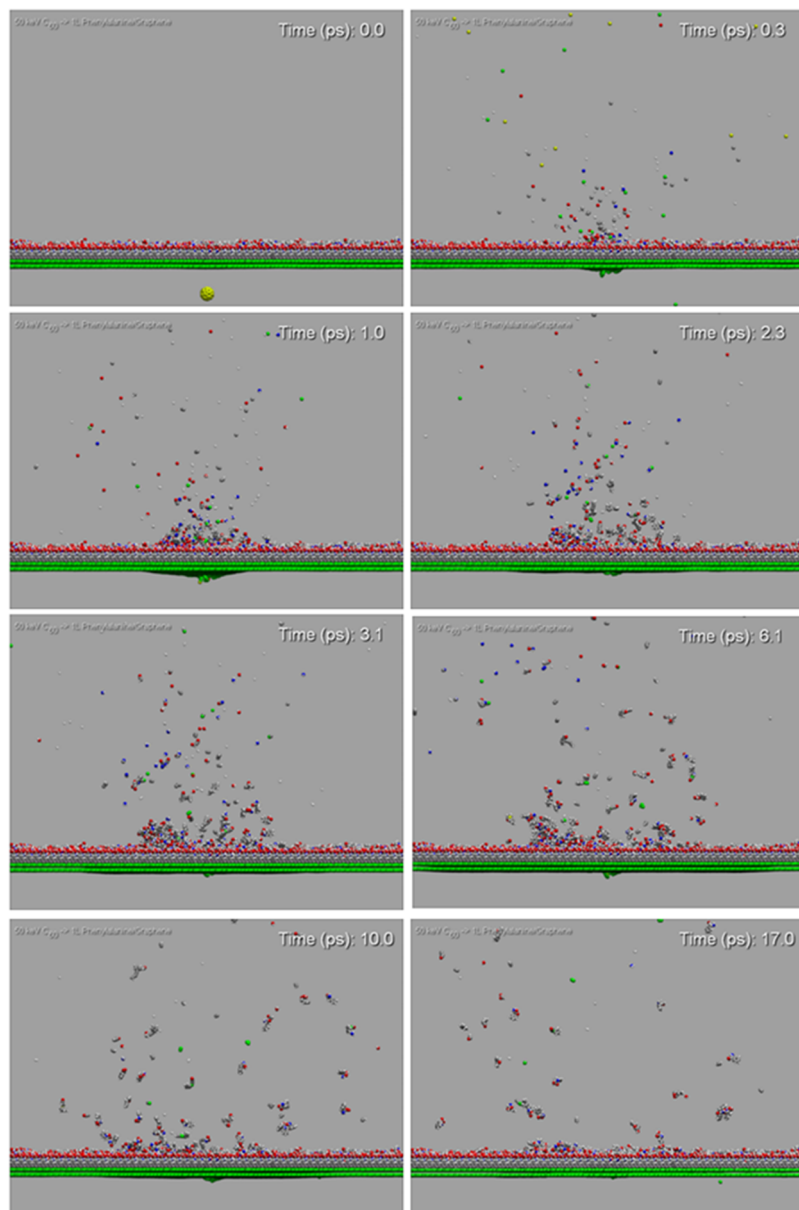


FIG. 8. Snapshots of the model system consisting of the single layer of phenylalanine molecules (1.1 nm) deposited on 2L graphene taken at various moments after 50 keV C_{60} impact—side view. The corresponding movie file is here. Multimedia view: <https://doi.org/10.1063/1.5021352.2>

radially from the hole [Fig. 7 (Multimedia view), screenshots for times 0.1 and 0.3 ps]. At the same time, this compression pushes the graphene membrane down. The molecular layer and graphene membrane are separated [Fig. 7 (Multimedia view), screenshots for times 0.6, 0.9, and 1.1 ps]. The pushed down graphene membrane is bent and stretched around the hole, thus accumulating potential energy. The result of the bending and stretching is an elastic movement of the membrane upward [Fig. 7 (Multimedia view), screenshots for times 1.5, 2.3, and 3.1 ps]. The accumulated potential energy is transformed into the kinetic energy of a correlated movement upward for membrane atoms. The membrane atoms interact with the atoms of Phe molecules and transfer the correlated momenta to them. Thus, the molecules eject without destruction. In other words, the membrane acts as a trampoline for the molecules. The ejection of molecules is clearly observable from the side view [Fig. 8 (Multimedia view)]. The screenshot for the time 1 ps [Fig. 8 (Multimedia view)] shows the strong

bending of the graphene membrane followed by the abundant trampoline ejection (1 ps–10 ps) of molecules and molecular clusters. Note that the emission/ejection of molecules is not effective in the reflection direction (impact on molecules first). This is due to the impact stimulated damage of molecules prior to the radial compression. This effect was investigated in Ref. 3 (MD simulations and experiments) for the single layer of C_{60} deposited on graphene.

A top view of the impact (Fig. 9) shows the evolution of the surface molecules around the impact site. This point evolves into a small graphene rupture of ~ 2 nm (time 0.1 ps after impact). The size of this rupture is reduced (self-healing effect¹³) within ~ 20 ps. The evolution of the area around the rupture shows a clearing of the graphene substrate by the processes of molecule ejection and radial compression. At the end of the ejection/compression, the area of graphene that is cleared of Phe molecules is ~ 6 nm in diameter. That area (at least in theory) corresponds to the

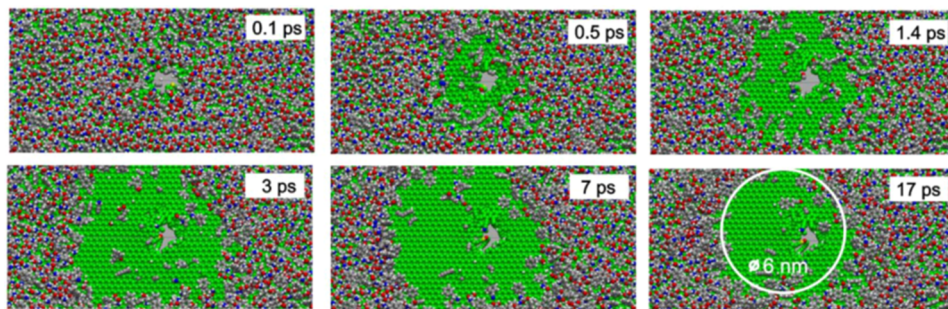


FIG. 9. Snapshots of the model system consisting of phenylalanine molecules deposited on 2L graphene taken at various moments after 50 keV C_{60} impact—top view. White circle marks dimension of the area cleared of organic molecules.

probing surface area for a single impact of 50 keV C_{60} projectile.

Phenylalanine monolayer on graphite

For comparison, we consider now molecule ejection and molecular ion emission from a single molecular layer deposited on pyrolytic graphite (Fig. 4). The yield of

0.15 ions/impact is comparable to the yield of $(D8Phe-H)^-$ emitted from the monolayer deposited on graphene (0.1 ions/impact). The MD simulations show that the critical process, which regulates the abundance of the ejecta, is a correlated upward movement of topmost graphite layers (Figs. 10 and 11) (Multimedia view). Figure 10 (Multimedia view) and the corresponding movie show the cut view, and Fig. 11 (Multimedia view) shows the side view.

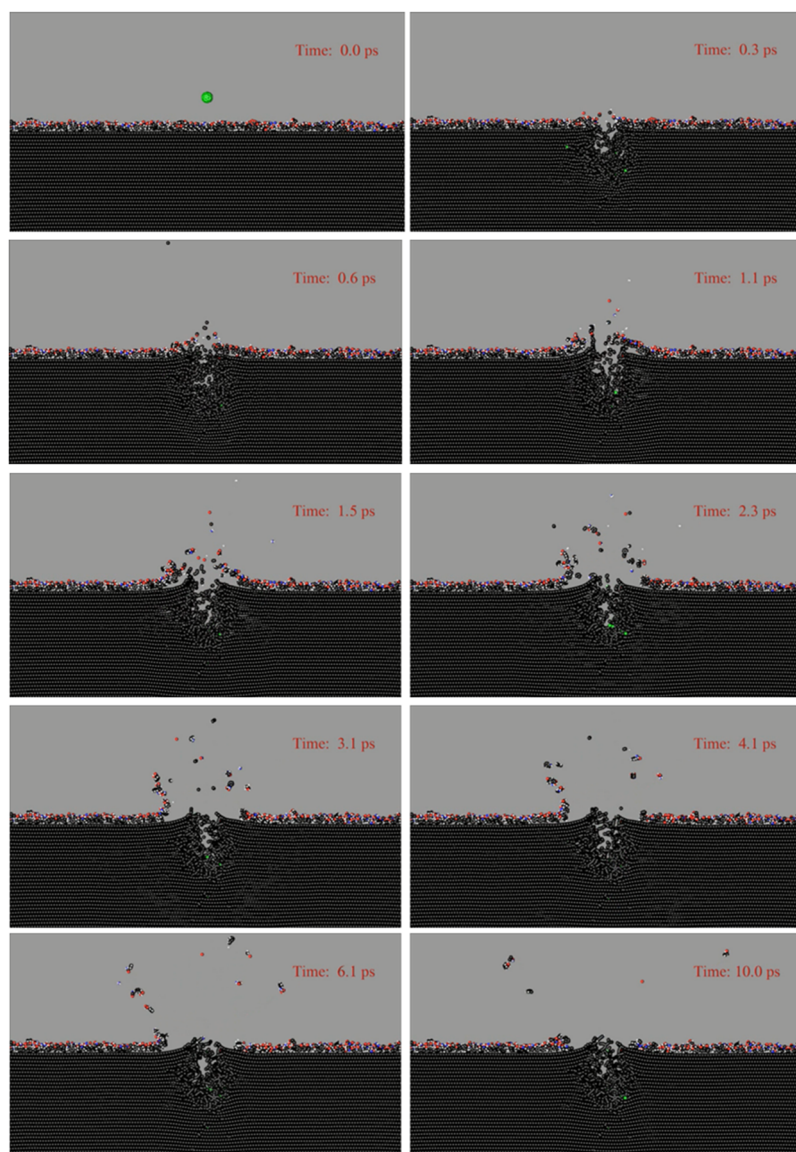


FIG. 10. Snapshots of the model system consisting of the single layer of phenylalanine molecules (1.1 nm) deposited on graphite taken at various moments after 50 keV C_{60} impact—cross-sectional view (slice 10 Å wide centered at the projectile impact point). The corresponding movie file is here. Multimedia view: <https://doi.org/10.1063/1.5021352.3>

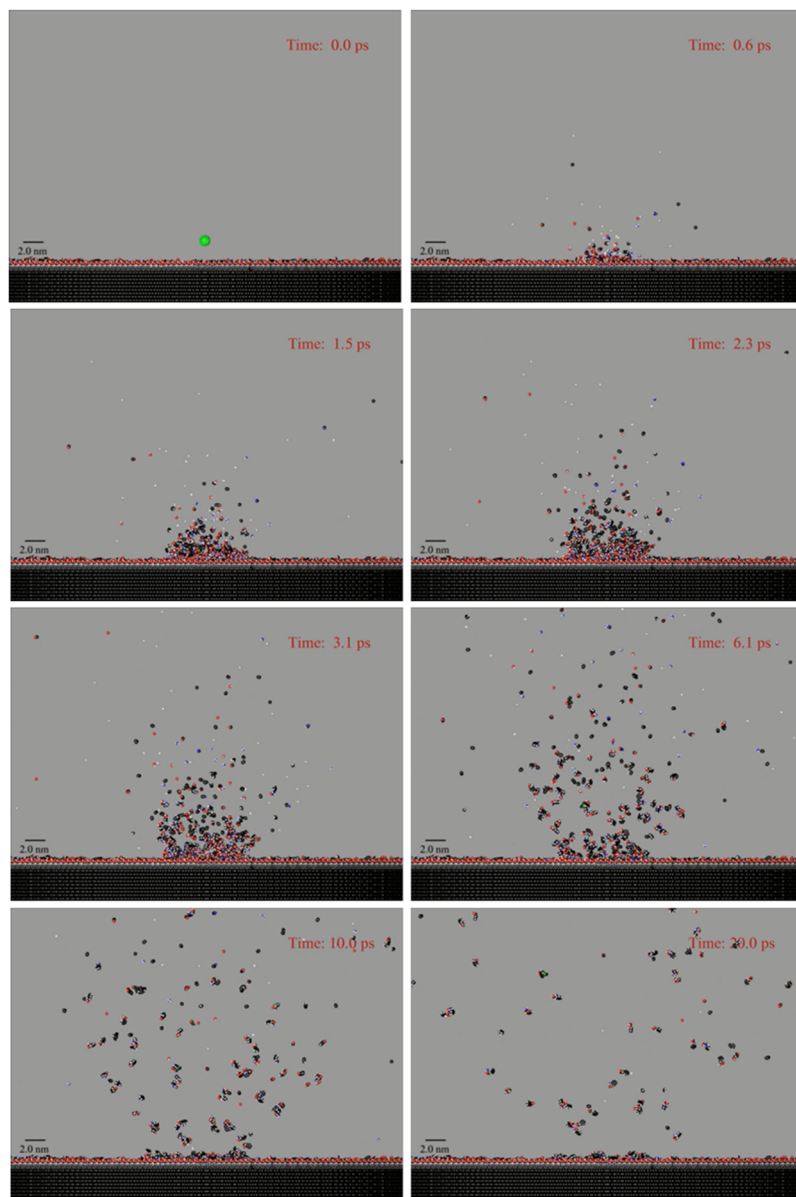


FIG. 11. Snapshots of the model system consisting of the single layer of phenylalanine molecules (1.1 nm) deposited on graphite taken at various moments after 50 keV C_{60} impact—side view. The corresponding movie file is here. Multimedia view: <https://doi.org/10.1063/1.5021352.4>

The detailed scenario is as follows: After impact [Fig. 10 (Multimedia view), screenshots for times 0.3 and 0.6 ps], the projectile atoms and fast recoiling atoms deliver the energy into the depth of graphite without strong damage to the surface layers of the analyte and graphite due to the latter's layer structure.

The result of the energy deposition is a high density collision cascade to a depth of ~ 5 nm (~ 15 graphite layers). The matter at this depth expands radially as seen in the deformation of the periphery graphite layers [Fig. 10 (Multimedia view), screenshots for times 1.1 and 1.5 ps]. At the same time, the expanding volume stimulates the collective movement of the topmost graphite layers upward. This movement transfers the correlated momenta to surface molecules, which eject without destruction [Figs. 10 and 11 (Multimedia view), screenshots for times 1.5, 2.3, and 3.1 ps].

The actual ejection mechanisms are similar for molecular layers on graphite or graphene. The graphene membrane as well as the topmost graphite layer acts as a trampoline for

the Phe molecules. The main difference is the initial projectile energy deposition for graphite and graphene prior to the molecule ejection. In the case of graphite, the high density collision cascade reaching the depth of ~ 5 nm stimulates in-depth radial expansion. The graphene evolution prior to the molecule ejection (more details are given above) does not involve a collision cascade.

In the case of bulk phenylalanine, the yield (0.13) of $(D8Phe-H)^-$ (Target III, Fig. 5) is again similar to the yields measured for ~ 1 nm layer of D8Phe deposited on graphene and graphite substrates (Figs. 3 and 4) despite the very different mechanisms of ejection/sputtering.

Bulk phenylalanine

For the bulk targets of organic molecules (weakly bonded molecular solids),¹⁴ the sputtering process has been extensively investigated.^{2,9,15,16} The abundant sputtering arises from the high density collision cascades that develop a crater in

the weakly bonded solid. The projectile impact at the surface creates an energized region primarily composed of molecular fragments.⁹ Expansion of this region stimulates molecular desorption at off-normal angles and high kinetic energy by means of fluid flow.¹⁵ Upon expansion of the region, molecules with low kinetic energy begin to desorb over all angles due to effusive-type motions.^{9,15} The periphery of the crater is responsible for the abundant sputtering of molecules and molecular clusters.⁹ Indeed, despite the similar yields (Targets I–III, Figs. 3–5), the shapes of the peaks of $(\text{D8Phe-H})^-$ are different. The right part of the peak (Fig. 5) has an extended tail, which is due to the fragmentation of molecular cluster ions.¹⁷ The vibrationally excited parent molecular cluster ion of phenylalanine (for instance Phe dimer) undergoes a unimolecular fragmentation¹⁸ into a daughter Phe ion and a neutral molecule.

The fragmentation of the parent molecular cluster ions occurs in the electrostatic field between the target and the extraction electrode and hence leads to a lesser daughter ion acceleration. The deficit in kinetic energy of a daughter ion when apparent as a peak tail indicates that the fragmentation process is a frequent de-excitation pathway for the parent molecular cluster ions.

The situation is different in the case of a monolayer deposited on graphite, here the small number of molecules limits the formation of molecular clusters in the ejection area [Target II, Fig. 4 and Figs. 10 and 11 (Multimedia view)]. Indeed, there is no extended tail (Fig. 4). Interestingly, molecular cluster fragmentation is observed in the peak obtained from a single layer of molecules deposited on graphene (Fig. 3). The effect is due to the radial compression of the molecular layer, when the molecules are agglomerated into the thick rim [Figs. 7 and 8 (Multimedia view)]. The MD simulations of 50 keV C_{60} impacts on 10 layers of Phe molecules deposited on graphene demonstrate that this system can be considered as an analog of the bulk Phe crystal. The total yield of Phe molecules computed for this case (165 molecules as separate entities, plus 190 molecules as molecular clusters) is significantly larger than the yield of Phe molecules from 1 layer of Phe deposited on graphene (9 molecules/impact).

Kinetic energy distributions

The shape of the low mass side of the $(\text{D8Phe-H})^-$ peak corresponds to the initial kinetic energy distribution of ejecta. Using the procedure referred to earlier, the peak shapes were converted into the kinetic energy distribution for all targets (Fig. 12). The distributions show that most of the molecular ions have low kinetic energies (0.01–0.1 eV range). This feature corroborates the mechanisms of a gentle ejection described above. However some molecular ions still have high kinetic energies (~ 10 eV), which are higher than the bond energies in the organic molecules. The molecular ejecta can acquire high translational velocities and survive, if the atom's momenta are correlated during the ejection. An oscillating membrane experiences up/down movement with frontal acceleration/deceleration, thus the membrane provides the correlated momenta (trampoline mechanism) that give some molecules an energetic push. The number of ejected molecules

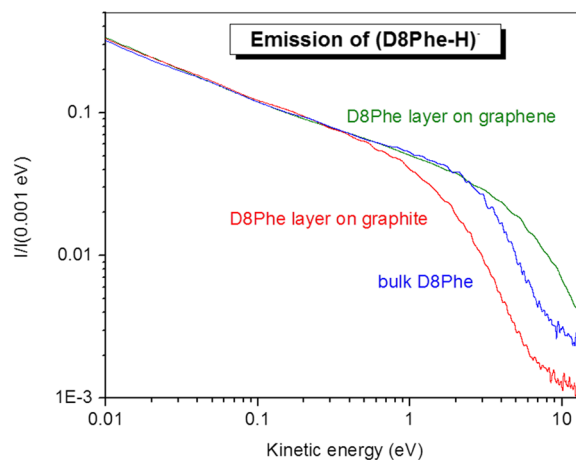


FIG. 12. Kinetic energy distributions measured for the molecular ions $(\text{D8Phe-H})^-$ emitted from: the single molecular layer of D8Phe deposited on 2-layer graphene (green color, Target I), the single molecular layer of D8Phe deposited on pyrolytic graphite (red color, Target II) and bulk D8Phe (blue color, Target III). The energy distributions at the high energy tails (> 10 eV) are not shown as they are distorted by an overlap with the small peaks of $(\text{D7Phe-H})^-$ ions. A small amount of D7Phe molecules are generated during the molecule deposition at the graphene surface.

at the peak velocity of the system molecule/membrane is small. Their probability of ionization though should be high as fast molecular ions pass the critical distance of electron tunneling within shorter time from ejection, thus having a lower probability of neutralization.¹⁹

Again most molecules have low kinetic energy, thus the low translational velocities do not increase the ionization probability. The high ionization probability of these molecules can be explained with the model of thermalized excitation.²⁰

Ionization

The ionization probability of molecules can be estimated from the experimental yields of ions and yields of neutral molecules from MD simulations as follows:

$$P_{\text{Phe}}^{(\text{exp})} = \frac{Y_{\text{Phe}}^-}{Y_{\text{Phe}}^0} \cdot \frac{1}{x}, \quad (8)$$

where Y_{Phe}^- is the yield of emitted $(\text{D8Phe-H})^-$ ions (measured experimentally), Y_{Phe}^0 is the yield of ejected Phe molecules (MD simulations) and $x \approx 0.5$ is the transmission/detection efficiency of the mass-spectrometer.

The yield of intact neutral molecules of Phe computed by MD is 9 molecules/impact for the Target I (the molecular layer of D8Phe deposited on graphene). Taking into account that the measured yield of $(\text{D8Phe-H})^-$ is 0.1, we infer an ionization probability (PI) of ~ 0.02 . A high PI = 0.2 is observed for the molecular fragment CN^- . The ionization probability for the Target III (bulk Phe) is significantly smaller. The measured yield of $(\text{D8Phe-H})^-$ is 0.13, and the computed by MD total yield of Phe is 355 molecules/impact, thus the PI $\sim 7 \cdot 10^{-4}$ only.

We have shown previously that for the emission of carbon cluster ions from 4-layer graphene³ as well as for the emission of C_{60}^- from a single layer of C_{60} deposited on graphene,⁴ the relevant mechanism of ionization is that of electron tunneling. The vibrationally excited graphene has an average electron

temperature of 3700 K at the rim at the time of the tunneling process.³ We can estimate within the framework of the adiabatic limit of the thermalized excitation model,¹⁹ the ionization probability of the Phe molecules

$$P_{\text{Phe}}^{(T)} = \left(\frac{Z^-}{Z^0} \right) \exp \left[- \frac{(\varphi - A - \delta_{ic})}{F(kT_e)} \right], \quad (9)$$

where T_e is the average electron temperature of the rim around the graphene hole at the time of the tunneling process, δ_{ic} is the image charge correction factor (set to zero here) and Z^- along with Z^0 are the partition functions of emitted C ions and neutrals at T_e . The work function of the rim is unknown. As an estimate, we can take the value of the work function of the free standing pristine graphene ($\varphi = 4.5$ eV). The electron affinity of the Phe molecule is in a range 3.2–3.5 eV,²⁰ thus taking the value of $T_e = 3700$ K from Ref. 3 one can estimate the ionization probability as $P_{\text{Phe}}^{(T)} \sim 0.02 - 0.04$. These values are consistent with the experimental value of 0.02. After ionization, the Phe⁻ molecule experiences a prompt fragmentation into the deprotonated negative ion, (D8Phe-H)⁻,^{21,22} thus the mass spectra contain (D8Phe-H)⁻ only. The formation of deprotonated negatively charged amino acids has previously been observed in the studies on the dissociative electron attachment.^{22–24} The difference with the experiment presented here is the nature of electrons involved in the ionization (free electron capture versus electron tunneling from graphene to Phe). The particular mechanisms of the prompt deprotonation of negatively charged amino acids are under discussion^{22–24} (out of scope of the present study).

Another possible mechanism of ionization is a direct proton transfer exchange: The ions of molecular fragments (i.e., CN⁻) generated in the impact area interact with intact molecules from the rim. The proton exchange for the system, Phe molecule + CN⁻, is energetically favorable (the energy of 15.2 eV for CN⁻ protonation²⁵ toward the energy of 14.75 eV for Phe molecule deprotonation).²⁶ The CN ions themselves are ionized by the tunneling mechanism mentioned above ($EA_{\text{CN}} \sim 3.9$ eV), as well as by an electron exchange with interacting molecular fragments within the hot area of the impact, where the density of the fragments is high.

The ionization via proton exchange between Phe molecules and negative ions of small fragments should be relevant for the molecular ion emission from bulk molecular matter. A different path via electron exchange between the sputtered molecules is unlikely given the high activation energy barrier (~ 12 eV—sum of Phe molecule electron affinity²¹ and ionization potential²⁷). One should note that the electron tunneling process between the molecule and the graphene/graphite layer is different due to the metallic bond structure (free electrons in the conduction band) of the graphene/graphite. The barrier for tunneling is only ~ 1 eV [Eq. (9)]. The hypothesis of the proton exchange mechanism for bulk Phe is supported by the evidence of a large number of the daughter molecular ions, which originate via fragmentation of the molecular cluster ions (Fig. 4 and discussion above). The neutral molecular clusters have a large cross section of interaction with CN⁻. The ionized molecular ion clusters (proton exchange with CN⁻) are, at the same time, sufficiently vibrationally excited (low energy bonds between molecules) to

fragment within the short times (ns-ms interval).¹⁷ The daughter molecular ions appear as prominent fragmentation tails of (D8Phe-H)⁻ (Fig. 4).

CONCLUSION

The efficient emission of molecular ions stimulated by impacts of 50 keV C₆₀²⁺ on phenylalanine molecules deposited as a single molecular layer on graphene was investigated experimentally. The abundant ion emission can be explained with insight from MD simulations showing a radial compression of the deposit combined with an oscillating movement of the graphene. The result is a “trampoline-like” ejection of molecules and molecular fragments. MD simulations confirm the experimental observation of emission of high kinetic energy molecular ions via the trampoline effect. We show that graphene enhances a probability of ionization for ejected molecules. We postulate that the high rate of negative ionization is due to electron tunneling from graphene to phenylalanine. A recently developed laser post-ionization, LPI, was applied on organic molecules of guanine and coronene, which were sputtered by 40 keV C₆₀⁺ bombardment from bulk targets^{28,29}. The LPI approach has yielded experimental positive ionization probabilities of $\sim 10^{-3}$ which may be compared with the 7×10^{-4} estimated for the molecules sputtered from bulk phenylalanine reported here. It will be interesting to compare on a broader range of compounds the experimental ionization probability measurements via LPI with the estimate involving data from MD simulations.

The trampoline ejection combined with efficient ionization generates molecular ion yields from monolayers of phenylalanine on graphene or graphite similar to those from a bulk analyte target. The similarity may be a fortuitous outcome of our experimental conditions. To advance our insight into the differences of projectile energy deposition in 2D and 3D targets, we plan experiments with varying projectile impact energies. Our observation shows that the deposition of energy into the 2D-like electron-rich atomic layer enhances the analyte ion yield, a critical issue for secondary ion mass spectrometry. Put differently, the physical properties of the substrate are the key for maximizing ejection-ionization of monolayer deposits of weakly bonded moieties. The prime condition though, is that of the energy density that must be delivered in a sub-ps interval into the 2D solid. Future experiments focusing on projectile energy loss should provide insight into the energetics required for trampolining-ionization.

ACKNOWLEDGMENTS

This work was supported by the National Science Foundation under Grant No. CHE-1308312 and by the Polish National Science Center, Grant No. 2015/19/B/ST4/01892.

¹P. van der Heide, *Secondary Ion Mass Spectrometry: An Introduction to Principles and Practices* (John Wiley & Sons, Inc., Hoboken, New Jersey, 2014).

²R. Behrisch and W. Eckstein, *Sputtering by Particle Bombardment* (Springer-Verlag Berlin Heidelberg, 2007).

³S. V. Verkhoturov, S. Geng, B. Czerwinski, A. E. Young, A. Delcorte, and E. A. Schweikert, “Single impacts of keV fullerene ions on free standing

- graphene: Emission of ions and electrons from confined volume," *J. Chem. Phys.* **143**, 164302 (2015).
- ⁴S. Sheng Geng, V. Verkhoturov, M. J. Eller, S. Della-Negra, and E. A. Schweikert, "The collision of a hypervelocity massive projectile with free-standing graphene: Investigation of secondary ion emission and projectile fragmentation," *J. Chem. Phys.* **146**, 054305 (2017).
- ⁵S. V. Verkhoturov, B. Czerwinski, D. S. Verkhoturov, S. Geng, A. Delcorte, and E. A. Schweikert, "Ejection-ionization of molecules from free standing graphene," *J. Chem. Phys.* **146**, 084308 (2017).
- ⁶S. V. Verkhoturov, M. J. Eller, R. D. Rickman, S. Della-Negra, and E. A. Schweikert, "Single impacts of C₆₀ on solids: Emission of electrons, ions and prospects for surface mapping," *J. Phys. Chem. C* **114**(12), 5637–5644 (2010).
- ⁷M. J. Eller, S. V. Verkhoturov, S. Della-Negra, and E. A. Schweikert, "SIMS instrumentation and methodology for mapping of co-localized molecules," *Rev. Sci. Instrum.* **84**(10), 103706-1–103706-7 (2013).
- ⁸R. D. Rickman, S. V. Verkhoturov, E. S. Parilis, and E. A. Schweikert, "Simultaneous ejection of two molecular ions from keV gold atomic and polyatomic projectile impacts," *Phys. Rev. Lett.* **92**, 047601-1–047601-4 (2004).
- ⁹B. J. Garrison and Z. Postawa, "Molecular dynamics simulations, the theoretical partner to dynamic cluster SIMS experiments," in *ToF-SIMS—Surface Analysis by Mass Spectrometry*, 2nd ed., edited by J. C. Vickerman and D. Briggs (IMP & Surface Spectra, Ltd., Chichester, Manchester, 2013), pp. 151–192, and references therein.
- ¹⁰J. F. Ziegler, J. P. Biersack, and U. Littmark, *The Stopping and Range of Ions in Solids* (Pergamon, New York, 1985).
- ¹¹Z. Postawa, B. Czerwinski, M. Szewczyk, E. J. Smiley, N. Winograd, and B. J. Garrison, "Enhancement of sputtering yields due to C₆₀ versus Ga bombardment of Ag{111} as explored by molecular dynamics simulations," *Anal. Chem.* **75**, 4402–4407 (2003).
- ¹²S. Plimpton, "Fast parallel algorithms for short-range molecular dynamics," *J. Comput. Phys.* **117**, 1 (1995).
- ¹³R. Zan, Q. M. Ramasse, U. Bangert, and K. S. Novoselov, "Graphene reknits its holes," *Nano Lett.* **12**, 3936–3940 (2012).
- ¹⁴M. Schwoerer and H. Ch. Wolf, *Organic Molecular Solids* (Wiley-VCH Verlag GmbH & Co., Weinheim, Germany, 2007).
- ¹⁵B. J. Garrison, Z. Postawa, K. E. Ryan, J. C. Vickerman, R. P. Webb, and N. Winograd, "Internal energy of molecules ejected due to energetic C₆₀ bombardment," *Anal. Chem.* **81**, 2260–2267 (2009).
- ¹⁶S. Sheraz nee Rabbani, I. B. Razo, T. Kohn, N. P. Lockyer, and J. C. Vickerman, "Enhancing ion yields in time-of-flight-secondary ion mass spectrometry: A comparative study of argon and water cluster primary beams," *Anal. Chem.* **87**, 2367–2374 (2015).
- ¹⁷J. D. DeBord, S. V. Verkhoturov, L. M. Perez, S. W. North, M. B. Hall, and E. A. Schweikert, "Measuring the internal energies of species emitted from hypervelocity nanoparticle impacts on surfaces using recalibrated benzylpyridinium probe ions," *J. Chem. Phys.* **138**, 214301 (2013).
- ¹⁸A. Wucher, N. K. Dzhemilev, I. V. Veyovkin, and S. V. Verkhoturov, "Fragmentation lifetimes and the internal energy of sputtered clusters," *Nucl. Instrum. Methods Phys. Res., Sect. B* **149**, 285 (1999).
- ¹⁹M. L. Yu and N. D. Lang, "Mechanisms of atomic ion emission during sputtering," *Nucl. Instrum. Methods Phys. Res., Sect. B* **14**(4-6), 403–413 (1986).
- ²⁰Z. Sroubek, X. Chen, and J. A. Yarmoff, "Ion formation and kinetic electron emission during the impact of slow atomic metal particles on metal surfaces," *Phys. Rev. B* **73**(4), 045427-1–045427-8 (2006).
- ²¹Z. G. Keolopile, M. Gutowski, and M. Haranczyk, "Discovery of most stable structures of neutral and anionic phenylalanine through automated scanning of tautomeric and conformational spaces," *J. Chem. Theory Comput.* **9**, 4374–4381 (2013).
- ²²Y. V. Vasil'ev, B. J. Figard, D. F. Barofsky, and M. L. Deinzer, "Resonant electron capture by some amino acids esters," *Int. J. Mass Spectrom.* **268**, 106–121 (2007).
- ²³A. M. Scheer, P. Mozejko, G. A. Gallup, and P. D. Burrow, "Total dissociative electron attachment cross sections of selected amino acids," *J. Chem. Phys.* **126**, 174301 (2007).
- ²⁴S. Denifl, H. D. Flosadóttir, A. Edtbauer, O. Ingólfsson, T. D. Märk, and P. Scheier, "A detailed study on the decomposition pathways of the amino acid valine upon dissociative electron attachment," *Eur. Phys. J. D* **60**, 37–44 (2010).
- ²⁵F. Ahu Akin and K. M. Ervin, "Collision-induced dissociation of HS⁻(HCN): Unsymmetrical hydrogen bonding in a proton-bound dimer anion," *J. Phys. Chem. A* **110**, 1342–1349 (2006).
- ²⁶C. M. Jones, M. Bernier, E. Carson, K. E. Colyer, R. Metz, A. Pawlow, E. D. Wischow, I. Webb, E. J. Andriole, and J. C. Poutsma, "Gas-phase acidities of the 20 protein amino acids," *Int. J. Mass Spectrom.* **267**, 54–62 (2007).
- ²⁷K. T. Lee, J. Sung, K. J. Lee, S. K. Kim, and Y. D. Park, "Conformation-dependent ionization of L-phenylalanine: Structures and energetics of cationic conformers," *Chem. Phys. Lett.* **368**, 262–268 (2003).
- ²⁸N. J. Popczun, L. Breuer, A. Wucher, and N. Winograd, "Ionization probability in molecular secondary ion mass spectrometry: Protonation efficiency of sputtered guanine molecules studied by laser postionization," *J. Phys. Chem. C* **121**, 8931–8937 (2017).
- ²⁹N. J. Popczun, L. Breuer, A. Wucher, and N. Winograd, "On the SIMS ionization probability of organic molecules," *J. Am. Soc. Mass Spectrom.* **28**, 1182 (2017).